Weak ferromagnetism and spin-glass behaviour of the n = 3 Ruddlesden-Popper compound $Ca_4Mn_3O_{10}$: a dc magnetization study

2000 J. Phys.: Condens. Matter 12 2505

(http://iopscience.iop.org/0953-8984/12/11/316)

J. Phys.: Condens. Matter **12** (2000) 2505–2524. Printed in the UK PII: S0953-8984(00)05204-8

Weak ferromagnetism and spin-glass behaviour of the $n = 3$ Ruddlesden–Popper compound $Ca_4Mn_3O_{10}$: a dc magnetization study

J Lago, P D Battle and M J Rosseinsky†

Inorganic Chemistry Laboratory, Department of Chemistry, University of Oxford, South Parks Road, Oxford OX1 3QR, UK

Received 15 June 1999, in final form 18 January 2000

Abstract. We present a detailed dc magnetization study of the compound $Ca_4Mn_3O_{10}$, which undergoes a transition into a G-type antiferromagnetic structure on cooling below 113.5 K. A series expansion analysis of the magnetic susceptibility shows the material behaves as a quasi-2D antiferromagnet in the temperature regime above T_N. This is corroborated by the analysis of the thermal evolution of the spontaneous magnetization obtained from neutron diffraction data. The antiferromagnetic transition is accompanied by the appearance at non-zero field of a net ferromagnetic moment of the order of 10^{-3} μ_B. This parasitic ferromagnetism is ascribed to a Dzyaloshinskii–Moriya term arising from the orthorhombic distortion of the crystal structure. The resulting weak ferromagnetic component in each MnO_2 layer is hidden at zero field but an applied magnetic field induces a spin-flop transition to a phase with a net magnetization. A non-zero moment is observed at temperatures well above the antiferromagnetic transition and may be responsible for the negative magnetoresistance, which persists to >200 K. The behaviour below T_N is dependent on the annealing treatment of the sample. Thermoremanent magnetization (TRM) measurements indicate a complex behaviour below the transition. TRM decay curves at low temperatures have been fitted to a stretched exponential function characteristic of spin glasses. The origin of this disordered behaviour may lie in the inhomogeneous distribution of the distortion that gives rise to the weak ferromagnetic phase, or in the detailed nature of that phase.

1. Introduction

The discovery [1, 2] of colossal magnetoresistance (CMR) in manganese oxides with the perovskite structure, $Ln_{1-x}A_xMnO_3$ (Ln being a rare-earth ion and A an alkaline-earth cation), renewed interest in the magnetism and magnetotransport behaviour of these materials, whose properties were first described almost 50 years ago [3, 4]. In these systems, substitution of the lanthanide sites with alkaline-earth cations introduces holes in the e_g band (i.e. a non-integral oxidation state (Mn^{3+}/Mn^{4+}) of manganese) which leads to both ferromagnetism and metallic conductivity. Double exchange [5] is thus thought to be the basic mechanism underlying the observed CMR effect although it alone is not sufficient to give a global explanation of the phenomenon [6–8]. In fact, experiments on the pyrochlore $Tl_2Mn_2O_7$ (Mn^{4+}) have demonstrated that CMR can occur even in the absence of detectable mixed valence [9, 10].

Attention soon focused on the $n = 2$ members of the Ruddlesden–Popper (RP) series [11], $(Ln, A)_{n+1}Mn_nO_{3_{n+1}}$ after the report of giant magnetoresistance (GMR) in single crystals of $(La_{0.4}Sr_{0.6})_3Mn_2O_7$ [12–14]. The Ruddlesden–Popper phases provide an invaluable

† Present address: Department of Chemistry, University of Liverpool, Liverpool L69 7ZD, UK.

0953-8984/00/112505+20$30.00

experimental model in which to study the effect of dimensionality of the magnetic lattice on the CMR effect. They consist of perovskite blocks of n layers of corner-sharing MnO_6 octahedra with neighbouring blocks separated by an (Ln, A)O rock-salt layer. The introduction of the rock-salt layer increases the number of bridging oxygens in the exchange pathway along the z-axis, thus causing a decrease in the value of the exchange constant in that direction. This produces an anisotropic reduction in the 3d bandwidth and hence modifies the magnetic and transport properties of these systems to an extent which depends on the value of n. In the $n = \infty$ $Ln_{1-x}A_xMnO_3$ systems CMR is generally constrained to a narrow region around the ferromagnetic transition, which is accompanied by an insulator to metal transition. For the lower n members of the series the observed behaviour is more varied. CMR has recently been demonstrated for the $n = 1$ members $Ca_{2-x}Ln_xMnO_4$ (Ln = Nd, Pr) [15]. For $(La_{0.4}Sr_{0.6})_3Mn_2O_7$ large magnetoresistance ratios are observed in the vicinity of the Curie temperature [12], whereas for other $n = 2$ systems CMR is observed over a wide temperature range below the ferromagnetic transition [16–18] or even without the onset of long-range ferromagnetism [19–21].

Less work has been done on the $n = 3$ RP phases. Here we report the results of dc magnetization measurements on the $n = 3$ member of the undoped $Ca_{n+1}Mn_nO_{3n+1}$ series, $Ca_4Mn_3O_{10}$. The members of this series contain manganese (+IV) and, in agreement with the Goodenough–Kanamori rules [22, 23], they show an antiferromagnetic spin arrangement [24], as predicted for a superexchange interaction between neighbouring Mn^{4+} t_{2g} electrons bridged by oxygen p_π orbitals. This makes them poor candidates for CMR through the conventional double exchange mechanism. Attempts have been made to dope the $n = 3$ member with La in order to induce mixed valence but only small doping levels have been reported to date in bulk samples [25, 26]. However, magnetoresistance ratios of up to 60% have been claimed in $La_{2.1}Ca_{1.9}Mn_3O_{10}$ thin films [27, 28]. The parent Mn(IV) phase itself displays magnetoresistance ratios of up to 40% [29]. Weak ferromagnetism in $Ca_4Mn_3O_{10}$ and $CaMnO_3$ was first reported by MacChesney *et al* [24], who, despite not giving an explanation for its origin, discarded the presence of impurities or oxygen deficiency as the origin of the thermomagnetic behaviour of these compounds. More recently, Briatico *et al* [30] studied the magnetic and electrical properties of $CaMnO_{3-\delta}$ ($\delta \leqslant 0.33$). They did not find any relationship between the conductivity of samples with different oxygen content and the weak ferromagnetism (WFM) observed in all of them, and thus concluded that the latter does not seem to be connected to the double-exchange (DE) mechanism.

Figure 1(a) shows the crystal structure of $Ca_4Mn_3O_{10}$ at room temperature. Previous neutron diffraction studies of this compound [31] have shown that it adopts an orthorhombically distorted structure (space group $Pbca$ $a = 5.265\,57(12)$, $b = 5.260\,39(11)$, $c = 26.8276(5)$ Å) with G-type [32] antiferromagnetic spin ordering within the perovskite blocks (figure 1(b)). However, dc magnetization measurements show the onset of a weak ferromagnetic moment at $T_N = 113.5$ K which decreases after reaching saturation. Muon-spin relaxation (μSR) studies [29] have shown evidence for a complex ground state below the ordering temperature, as the oscillations usually associated with antiferromagnetic long-range ordering were not observed. In order to understand the nature of the low-temperature magnetic phase we have measured the magnetization as a function of applied magnetic field and the time decay of the thermoremanent magnetization (TRM). The resulting picture, characterized by a spin-glass-type behaviour at low temperatures, can be discussed either as a result of the transition from an antiferromagnetic-to-spin-flop-to-saturated paramagnetic phase or within a picture of weak ferromagnetic clusters arising from inhomogeneously distributed distortions of the crystallographic structure. The latter explanation has been proposed in some cuprate systems [33–35]. The magnetization above the Néel temperature is discussed in terms of the

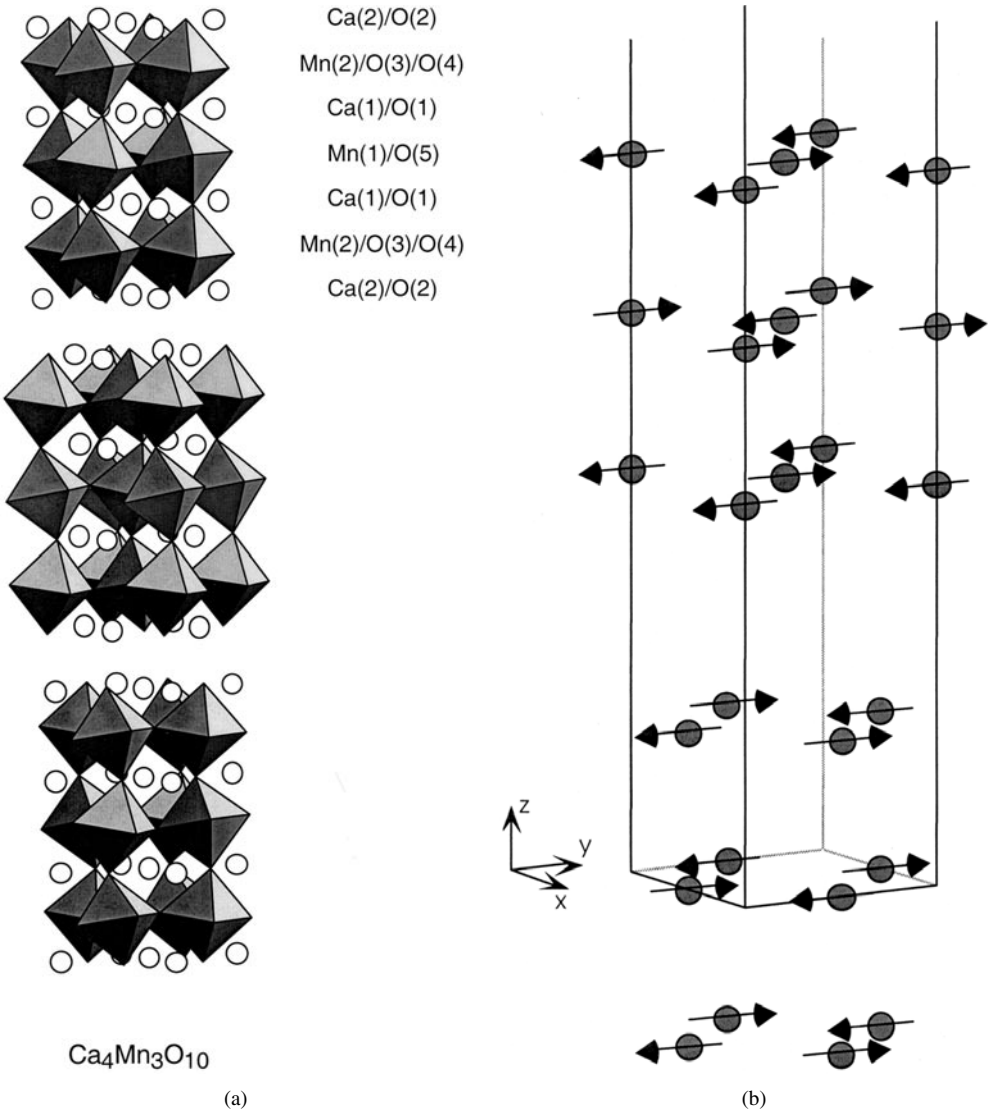

Figure 1. (a) Crystal structure of $Ca_4Mn_3O_{10}$. (b) Magnetic structure of $Ca_4Mn_3O_{10}$.

low dimensionality of the system. We postulate the existence above the transition temperature of antiferromagnetically correlated regions within the *ab* planes which accommodate the weak ferromagnetic moments found at temperatures as high as 225 K.

2. Experiment

Polycrystalline samples of $Ca_4Mn_3O_{10}$ were prepared under flowing oxygen by the standard ceramic method with firing temperatures of up to 1330 °C. Details of the synthetic method have already been described in a previous publication [31]. Further experiments were carried out on one of these as-synthesized samples which will be called sample A. A second batch of sample, B, was prepared by annealing the material obtained at ambient pressure at 500 °C under a high

pressure of oxygen ($\widetilde{=}$ 800 atm) in order to produce full oxygen stoichiometry. Pressure was generated using a Fluitron diaphragm compressor. The sample was wrapped in gold foil and contained in a René 41 pressure vessel. Attempts were made to determine the exact oxygen content by means of iodometric titration and thermogravimetric analysis but the results were inconclusive. Phase purity was established using x-ray and neutron diffraction techniques, as outlined previously [31]. The crystal structure was determined from neutron data collected at 5 K and room temperature on the powder diffractometer HRPD at ISIS, RAL. Neutron powder diffraction data at long d-spacings were collected to search for magnetic reflections for sample A. Measurements were performed on both the IRIS time-of-flight diffractometer at ISIS at 5 K over the range $2.1 \leqslant d$ (Å) $\leqslant 5.5$ and at temperatures ranging from 10 to 135 K over the range $3.3 \leqslant d$ (Å) $\leqslant 5.5$, and on the D1B constant wavelength diffractometer (ILL, $\lambda = 2.5219$ Å) at 1.5 K over the range $1.7 \leqslant d$ (Å) $\leqslant 7.2$.

Magnetization data were collected in a Quantum Design MPMS SQUID magnetometer. Both zero-field-cooled (ZFC) and field-cooled (FC) curves were recorded while warming the sample to room temperature after cooling it to 5 K. For the field-cooled measurements the same applied field used for collecting ZFC data was retained on cooling. Measurements of the time decay of the thermoremanent magnetization (TRM) were performed by cooling the sample from room temperature to the experimental temperature under an applied field. Fields of 0.02 and 0.1 T were used. After a 'waiting time' of 1000 s had elapsed at the measuring temperature, data were collected at regular intervals for over four hours.

3. Results and discussion

3.1. Weak ferromagnetism below T_N

Figures 2(a) and (b) show the temperature dependence of the molar magnetic susceptibility for samples A and B, respectively, under different applied fields. For both samples and in all fields, the FC magnetization curves show a sharp increase at a temperature of ∼115 K. The magnitude of the moment associated with this transition is, however, very small (of the order of 10^{-3} μ_B, from measurements of magnetization versus applied field) and thus cannot be ascribed to the onset of conventional 3D ferromagnetic ordering of the Mn^{IV} ions (3 μ_B). It has been previously demonstrated that $Ca_4Mn_3O_{10}$ orders antiferromagnetically below this temperature [24, 31]. The variation with temperature of the sublattice magnetization obtained by fitting the intensity of the 104 magnetic reflection in neutron diffraction data recorded on the IRIS diffractometer (Rutherford Appleton Laboratory) is displayed in figure 3. It clearly shows a sharp increase at $T_N \sim 113$ K in agreement with an antiferromagnetic transition.

The weak ferromagnetism is only apparent in the ZFC measurements (figure 2) for the highest value of the applied field, $B = 1$ T. Measurements in lower fields, 0.01 T for sample A and 0.1 T for sample B, show a sharp cusp characteristic of an antiferromagnetic transition occurring at the same temperature as the onset of weak ferromagnetism (WFM), indicating the link between the two phenomena. The inset in figure 2(a) shows an enlargement of the ZFC curve collected in a field of 0.01 T around the transition temperature. It clearly shows the cusp at T_N, which is partially hidden in the larger plot. Irreversible behaviour marked by the divergence of the FC and ZFC curves starts at the transition temperature for both samples.

The inverse susceptibility above the Néel temperature displays two distinct slopes for $T_N < T < 170$ K and $T > 180$ K. Attempts to fit the high-temperature data to a Curie–Weiss law yielded $\theta = -525$ K, consistent with strong antiferromagnetic coupling of the manganese ions and in agreement with the results of Fawcett *et al* [36], although true Curie–Weiss

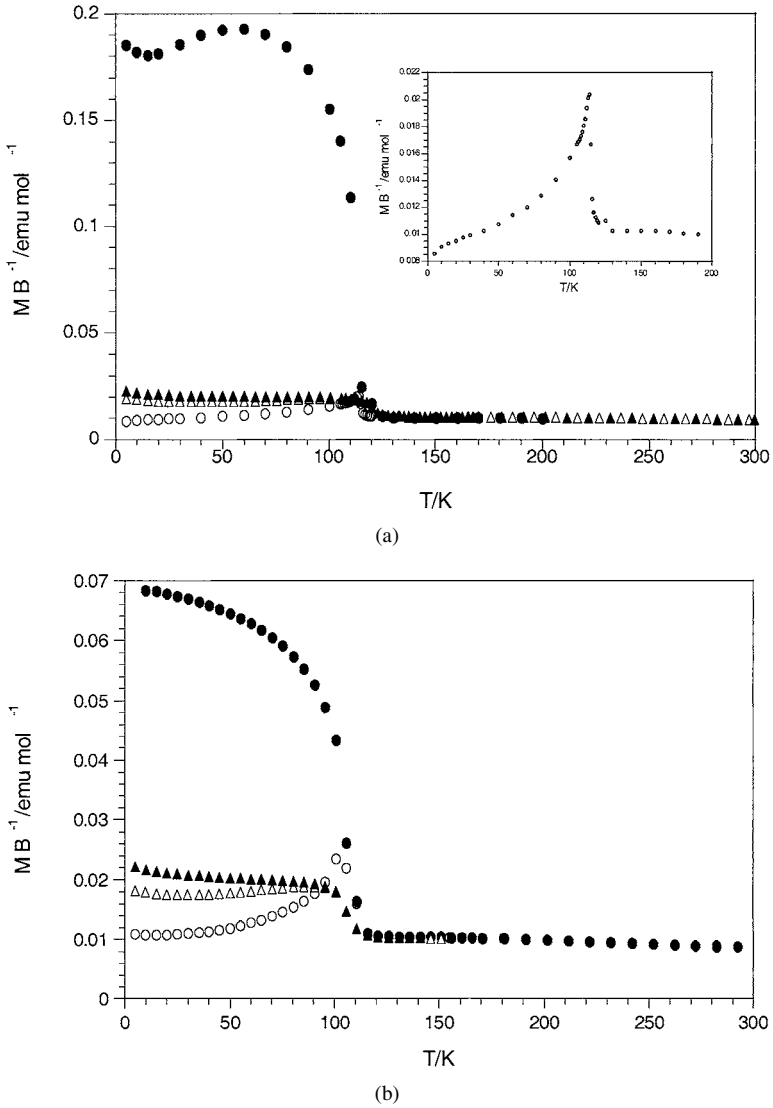

Figure 2. (a) Temperature dependence of the molar magnetic susceptibility for sample A under $B = 0.01$ T (circles) and 1 T (triangles). Filled and empty symbols are used to indicate field-cooled (FC) and zero-field-cooled (ZFC) data respectively. The inset shows an enlargement of the region around the transition temperature for the ZFC data collected in 0.01 T in order to show the cusp in susceptibility occurring at T_N. (b) Temperature dependence of the molar magnetic susceptibility for sample B under $B = 0.1$ T (circles) and 1 T (triangles). Filled and empty symbols are used to indicate field-cooled (FC) and zero-field-cooled (ZFC) data respectively.

behaviour will clearly not be observed in the measured temperature range. The fact that the same features were obtained for samples prepared under different synthetic conditions indicates the intrinsic nature of the observed features.

The small ferromagnetic component of the magnetization in the ordered state could in principle have two distinct explanations. In the hole-doped CMR manganites, in which mixed valence Mn^{3+}/Mn^{4+} occurs, ferromagnetism is explained within the framework of the DE

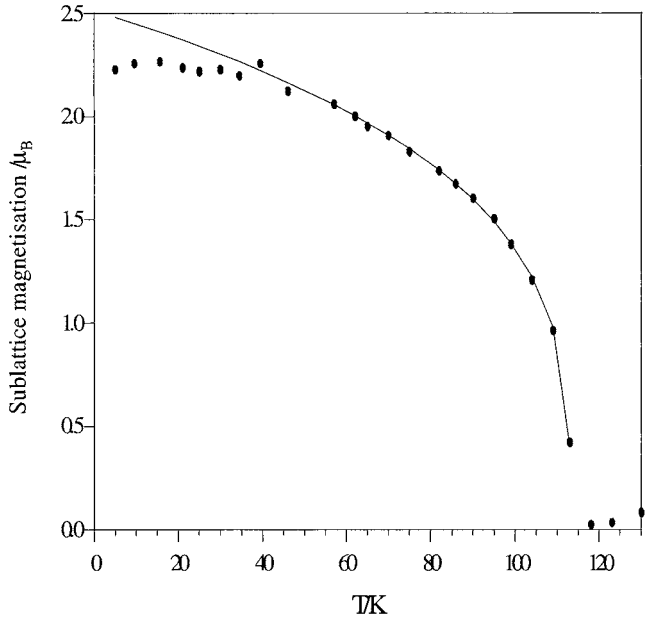

Figure 3. Thermal variation of the sublattice magnetization as obtained from refinement of the magnetic structure of $Ca_4Mn_3O_{10}$ from neutron powder diffraction data. The solid line represents the fit to a scaling power law $\mu = 2.514 \times (1 - T/113.23)^{0.286}$.

model [5], in which the mobile e_g electrons supplied by the Mn^{3+} ions ferromagnetically couple the localized t_{2g} spins of a Mn^{3+}–Mn^{4+} neighbouring pair. Maignan *et al* [37] have suggested a DE origin of the weak ferromagnetic component in $CaMnO_{3-\delta}$ ($\delta \leqslant 0.02$) as a result of the small deviation from the fully oxidized stoichiometry that introduces a small concentration of e_g electrons on the Mn^{4+} lattice. In view of the inconclusive oxygen analysis of the samples under study, we cannot in principle discard this explanation of the weak ferromagnetic moment (WFM) found in $Ca_4Mn_3O_{10}$. However, the refinement of the anion occupancy fractions from high-resolution neutron diffraction data failed to detect any deviation from unity for an A-type sample, thus indicating that the stoichiometry of this sample is very close to $Ca_4Mn_3O_{10}$. The unit-cell volume of this sample was found to be slightly larger than that of a high-pressure annealed sample (type B), implying a higher Mn^{4+} content for the latter and, hence, an even smaller deviation from the nominal stoichiometry [31]. In both cases, the refined unit-cell volume was smaller than that reported in [24] for $Ca_4Mn_3O_{9.96}$. Moreover, the thermally activated resistivity found for both the as-prepared and the annealed samples [29] suggest a system of localized spins in contrast to the metallic-like behaviour reported for $CaMnO_3$ by Maignan *et al* [37]. It seems reasonable to think that in such a system, a ferromagnetic component arising from double exchange involving Mn(III) centres associated with oxygen vacancies would be extremely dependent on the concentration of Mn(III) both in magnitude and onset temperature since, for the small oxygen substoichiometries assumed for our samples, a behaviour characteristic of short range (SRO) ferromagnetic clusters rather than true long range (LRO) ferromagnetic ordering would be expected. On the contrary, temperature-dependent magnetization measurements carried out on samples prepared under a variety of oxidizing conditions indicate that the magnetic transition temperature is invariant with the synthesis procedure. Similar behaviour is observed in the muon-spin relaxation data [29] where the

initial asymmetry is almost temperature independent down to T_N, at which point a large drop occurs, indicating a sharp thermodynamic transition rather than thermal evolution of ferromagnetic clusters. Isothermal magnetization curves also yield very similar values for the magnetic moment per manganese site for the two types of sample. We therefore conclude that, even assuming the existence of a small concentration of Mn^{3+} cations, these are not responsible, through the DE interaction, for the WFM component observed below the Néel temperature.

Weak ferromagnetism as an intrinsic property of $Ca_4Mn_3O_{10}$ can arise from a Dzyaloshinskii–Moriya (DM) term [38, 39] introduced by the orthorhombic distortion of the crystal structure. The DM term is responsible for canting the spins away from the direction of the staggered magnetization (which lies in the ab plane in $Ca_4Mn_3O_{10}$) and it is only allowed provided that the canted and uncanted structures contain the same symmetry elements, which, in general, is only possible for low crystal symmetry [40]. In $Ca_4Mn_3O_{10}$, the MnO_6 octahedra rotate about two perpendicular axes, [110] and [1$\bar{1}$0], in the ab plane causing the Mn–O–Mn bond angles to deviate from the ideal value of 180° [31]. This tilting removes the centre of inversion at the oxygen sites in the ab planes and thus allows a non-zero antisymmetric exchange term which gives rise to canting of spins in each MnO_2 plane. The resulting planar Hamiltonian can be expressed as

$$H = -1/2 \sum_{ij} J_{ij}(\vec{S}_i \cdot \vec{S}_j) - 1/2 \sum_{ij} \vec{D}_{ij} \cdot (\vec{S}_i \times \vec{S}_j) - g\mu_B H \sum_i \vec{S}_i \qquad (1)$$

where the second term is the DM interaction and the weak ferromagnetic moment arising from the DM interaction is given by $M = (\vec{D} \times \vec{l})/J$ where $\vec{l} = (\vec{M}_1 - \vec{M}_2)/2$ is the staggered magnetization and J is the isotropic exchange constant in the MnO_2 planes [41]. The WFM moment is therefore always perpendicular to $\vec{l}$ and $\vec{D}$. Our neutron diffraction data [31] show that $\vec{l}$ lies along the b direction. The direction of the DM vector could, in principle, be found from symmetry considerations using the rules given by Moriya [39]. However, this is not possible in the case of $Ca_4Mn_3O_{10}$ as none of the symmetry operations that indicate the direction of the DM vector are present within the specific tilting pattern found for this material. Thus we are not able to define the orientation of the weak ferromagnetic moment in the ac plane.

Assuming a classical spin model at zero temperature, the canting angle, ϕ, can be estimated from the ratio between the uniform and staggered magnetizations, $\vec{m} = (\vec{M}_1 + \vec{M}_2)/2$, and $\vec{l} = (\vec{M}_1 - \vec{M}_2)/2$ respectively where $\vec{M}_1$ and $\vec{M}_2$ and are the two sublattice magnetizations in the ab plane. The uniform magnetization represents the WFM component and can be calculated from the field dependence of the dc susceptibility. From data collected at 110 K we calculate a value of 0.005 μ_B. The staggered magnetization describes the AFM sublattice component and we calculate a value of 2.23 μ_B from refinement of neutron diffraction data [31]. This results in an experimental value of the canting angle of 0.13°. This value indicates the magnitude of the antisymmetric DM exchange compared to the average intraplanar exchange coupling, J, since [42]

$$\tan\phi = \langle D_{ij} \rangle / |J|. \qquad (2)$$

Taking $|J| = 19.7$ K from our calculations below, we obtain $\langle D_{ij} \rangle \sim 0.045$ K.

3.2. Magnetic dimensionality and behaviour above the transition temperature

The temperature dependence of the susceptibility above T_N for sample A is expanded and shown in figure 4. It is clear from direct inspection of the curve that the material does not display a simple Curie–Weiss paramagnetic behaviour in this temperature range. The analysis below suggests that the departure from CW behaviour arises from the two-dimensional character of

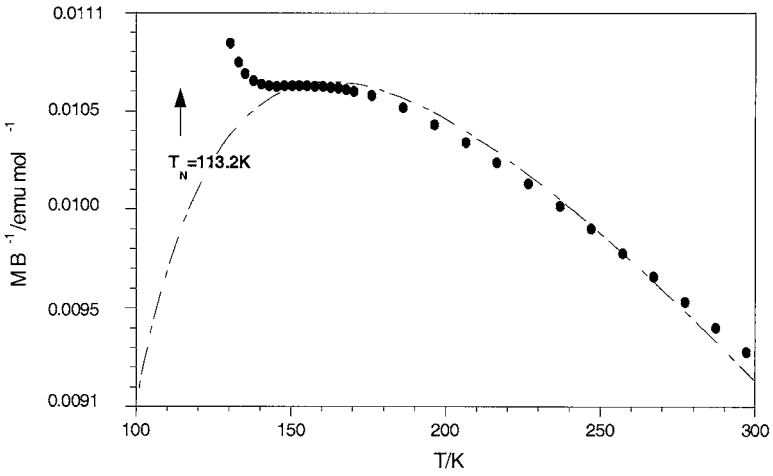

Figure 4. Thermal variation of the magnetic susceptibility above the Néel temperature for sample A. The dashed line is an attempt to fit the data to a high-temperature series expansion in powers of the reduced temperature, $\theta = k_B T/J$, using only the first six coefficients given in [44] for the quadratic Heisenberg antiferromagnet.

the spin system, with regions of antiferromagnetically correlated spins within the *ab* planes above T_N.

The occurrence of a broad maximum in χ at $T_{\max} > T_N$, centred at around 155 K for our material, together with a weak thermal variation of the susceptibility for temperatures above $T_{\max}$ (for $Ca_4Mn_3O_{10}$ the variation of χ between $T_{\max} \sim 155$ K and room temperature is only 11.6%, compared to ∼4% in Ca_2MnO_4 [43] and ∼35% calculated for a CW susceptibility in a spin-only Mn^{IV} system ($\mu = 3.87\ \mu_B$) with $\theta = T_N = 113.5$ K) is characteristic of two-dimensional antiferromagnetic systems [43, 44]. We have calculated $|J|/k_B \sim 19.7$ K from the value of T_{max} using the expression proposed by de Jongh for the quadratic layer antiferromagnet [45]. This value is in good agreement with the predicted increase in the intraplanar exchange constant with decreasing n in the series $Ca_{n+1}Mn_nO_{3n+1}$ [43, 46]. For the $n = \infty$ member, $CaMnO_3$, we obtain $|J|/k_B \sim 11.7$ K using the formula given by Rushbrooke and Wood [47–49] for a simple cubic antiferromagnet and taking $T_N = 123$ K [24], and a value of $|J|/k_B \cong 28.6$ K has been reported for Ca_2MnO_4 [45, 50]. This trend in J has been experimentally observed in other Mn^{IV} series [51] and implies an increase in the t_{2g}–O p_π–t_{2g} overlap integral as n decreases.

The dotted line in figure 4 represents an attempt to fit the experimental susceptibility data to a series expansion using the six first coefficients C_n given by Lines [44] for the square lattice Heisenberg antiferromagnet, leaving the gyromagnetic factor, g, and J/k_B as fitting parameters. The fit to

$$\frac{Ng^2\mu_B^2}{\chi J} = 3\theta + \sum_{n=0}^{\infty} \frac{C_n}{\theta^{n-1}} \tag{3}$$

where $\theta = k_B T/J$ is the reduced temperature, leads to $|J|/k_B \cong 41.1$ K [50] and a unrealistic value of $g \sim 3.3$. The use of the purely 2D model is consistent with the existence of a maximum in the susceptibility at $T \sim 155$ K and provides a qualitative picture of the behaviour above T_N. However, it does not give a good quantitative description. In layered materials with magnetic ions coupled by superexchange interactions, magnetic dimensionality is a function of the ratio

between the magnitudes of the intra- and interlayer coupling constants, J and J' respectively. The behaviour is effectively 2D when $J/J' \geqslant 10^2$ [45]. As a general rule, one can assume that each additional anion reduces the strength of the interaction along that path by a factor of 10^2 [45]. Thus, in $Ca_4Mn_3O_{10}$, with an extra bridging oxygen every three perovskite layers along c, a reduction in J' of less than two orders of magnitude from the value in the perovskite $CaMnO_3$ (pure 3D behaviour) is expected, that is, not sufficiently large to give rise to a true 2D behaviour. Therefore, the fit to a pure 2D model is far from being satisfactory. However, the reduction is large enough to lower the dimensionality of the system and give rise to the quasi-2D features we observe in the thermal variation of the susceptibility.

The temperature dependence of the sublattice magnetization obtained from the intensity of the 104 magnetic reflection is fitted to the scaling power law

$$M = M_0 \left(\frac{T_N - T}{T_N} \right)^{\beta} \tag{4}$$

in the reduced temperature range $0.035 \leqslant T^* \leqslant 0.24$ ($T^* = 1 - T/T_N$) in figure 3, yielding $\beta = 0.286$. A value of $\beta = 0.23$ has been theoretically predicted by Bramwell and Holdsworth [52, 53] for 2D XY systems in the 'subcritical' regime ($T^* > 0.01$) and, following previous indications by de Jongh and Miedema [45], the same authors have suggested that values of $\beta > 0.23$ are characteristic of behaviour intermediate between 2D and 3D [53, 54]. Data over a wider reduced temperature range are required for detailed comparison with theory.

3.3. Magnetization in the ordered state: field-induced nature of the WFM component

Whereas the onset of the weak ferromagnetic component occurs at the same temperature for the two samples, at temperatures below the transition the behaviour in low applied fields is strongly dependent on the synthetic conditions used for each sample. For sample B (figure 2(b)) the magnetization increases below T_N and saturates at low temperatures. In the case of sample A (figure 2(a)) the weak ferromagnetic moment decreases after reaching a maximum at ~70 K, only to increase again at $T \sim 20$ K. Under applied fields $B \geqslant 1$ T (for clarity only $\mu H_{appl} = 1$ T data are shown in figures 2(a) and 2(b)) the magnetization increases in the low-temperature region for both samples. In both cases, irreversible behaviour, marked by the divergence of the ZFC and FC curves, starts at the transition temperature and vanishes with increasing applied field.

Curves of magnetization versus field are displayed in figures 5(a) and (b) for sample A. Those of sample B are essentially the same. For measurements carried out at temperatures above the transition (figure 5(b)) we find a linear dependence on the applied field. However, for data collected at 140 K, subtracting the linear term $\chi_\infty B_{appl}$ from the magnetization measured after field-cooling the sample in $B_{appl} = 0.01$ T yields a curve which shows a very weak ferromagnetic moment ($M \cong 3 \times 10^{-5}\ \mu_B$) which saturates at $B_{appl} \cong 0.1$ T (figure 5(c)) (here $\chi_\infty(T) = \lim_{(H\to\infty)}(\mathrm{d}M/\mathrm{d}B)_T$ is the slope of the M–H curve at the high-field limit, where any ferromagnetic component is saturated). A similar result is obtained at 223 K although, in this case, the sample was cooled under a field of 5 T. At 300 K a slight departure from linearity is observed at small fields. Weak ferromagnetism at temperatures above T_N has been reported in Ln_2CuO_4 compounds (Ln = Y, Gd) for which ferromagnetic-like magnetization curves were found up to 50 K above the onset of AFM order [33, 34] and explained as the result of the stabilization of the weak ferromagnetic phase by the applied magnetic field. The role of the field in inducing the ferromagnetic ordering of the WFM moments at temperatures below T_N, which will be discussed below, together with the apparent saturation of the small moment found at high temperatures seems to support this explanation. The existence of

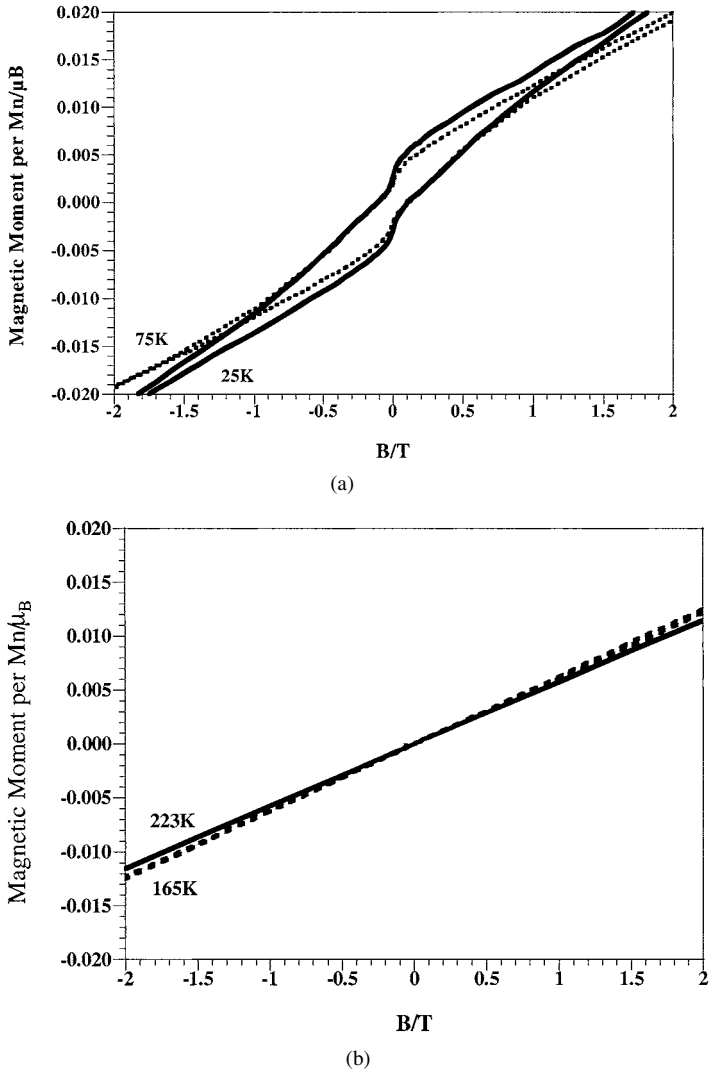

Figure 5. ZFC $M(H)$ isotherms for sample A at different temperatures below (a) and above (b) $T_N \sim 113$ K. The weak ferromagnetic component is clearly observed for temperatures below the transition temperature, whereas for $T \geqslant T_N$, a linear field dependence is found on a first approximation. Figure (c) shows the field dependence of the FC magnetization ($B = 0.01$ T) at 140 K expressed as magnetic moment per manganese atom once the linear part $\chi_\infty B$ has been subtracted from the raw data. The error bars show the standard deviation associated with each experimental point. This figure shows that a weak ferromagnetic component exists well above T_N.

weak ferromagnetism at high temperature could have important implications for the negative magnetoresistive behaviour found for this compound (up to 40% in an applied field of 14 T at 60 K), which becomes apparent at ~200 K [29].

Figure 6 shows the hysteresis loops obtained in ZFC conditions for three different temperatures below T_N once the linear contribution arising from the main antiferromagnetic framework has been subtracted as described above. These measurements corroborate the presence of irreversibility up to the transition temperature. The weak ferromagnetic component

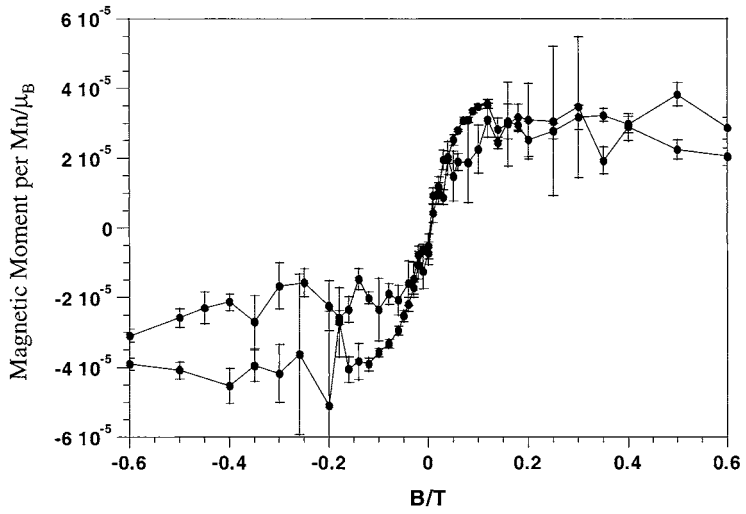

(c)

Figure 5. (Continued)

saturates at a value of $\sim$5–6 $\times$ 10^{-3} μ_B per manganese for the three measured temperatures although a reduction in this component with increasing magnetic field is observed in the curve at 25 K. This is a consequence of the method used to obtain the curves. The most striking feature of these measurements is, however, the narrowing along the magnetization axis that occurs at low values of B_{appl}. Although observed for the whole temperature range below T_N, this behaviour becomes more noticeable upon cooling. We interpret this behaviour as a result of a spin-flop (SF) transition taking place at a critical value of the field that varies with temperature and remains finite up to the Néel point where it vanishes.

In order to clarify the exact nature of this transition we have plotted in figure 7 the initial ZFC magnetization of sample B collected at 5 K together with the differential susceptibility, $\chi_d \equiv \mathrm{d}M/\mathrm{d}B$, obtained numerically from the same data. A sharp increase of magnetization accompanied by a peak in χ_d is observed at a value of applied field of around 0.5 T. This peak leads to a region where the differential susceptibility remains constant (i.e. linear increase of the magnetization) before dropping for $B_{appl} \geqslant 3$ T. The drop observed in the magnetization in the low- and high-field regions is just an artefact arising from the subtraction of the linear AF term. However, the differential susceptibility is not affected by the subtraction of the constant term and thus displays the true evolution of the WFM component. Overall, the observed field-dependent behaviour of the WFM component is that predicted by a mean field theory for a Heisenberg antiferromagnetic system with weak anisotropy [45]; when a field is applied parallel to the preferred axis of antiferromagnetic ordering, the moments tend to align perpendicular to this axis. At low values of B_{appl}, the anisotropy field that determines the preferred orientation prevents this. However, at a certain critical value the applied field overcomes the anisotropy and a spin-flop transition takes place. The moments orient themselves perpendicular to B_{appl}. A further increase in the field produces a gradual rotation of the spins until at a second critical value they lie parallel along the easy axis and a so-called 'saturated paramagnetic' [45] (SP) phase is entered. The first transition from the antiferromagnetic to the spin flop phase is of first order [45] and so it is characterized by a discontinuity in the magnetization and a sharp peak in its first derivative, as observed in our experimental data. The first-order character

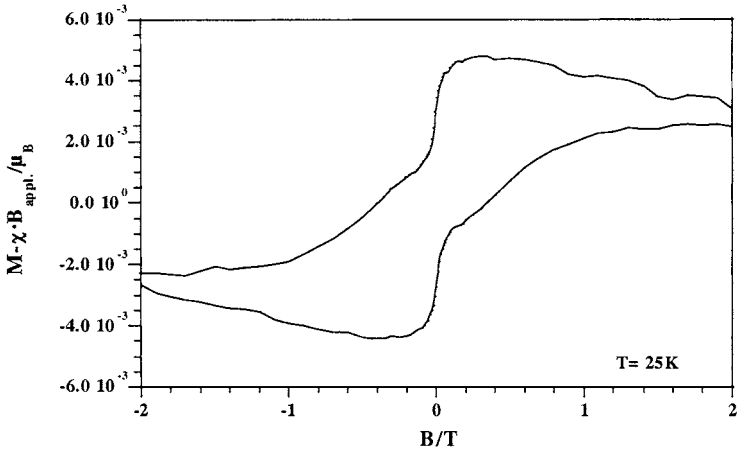

(a)

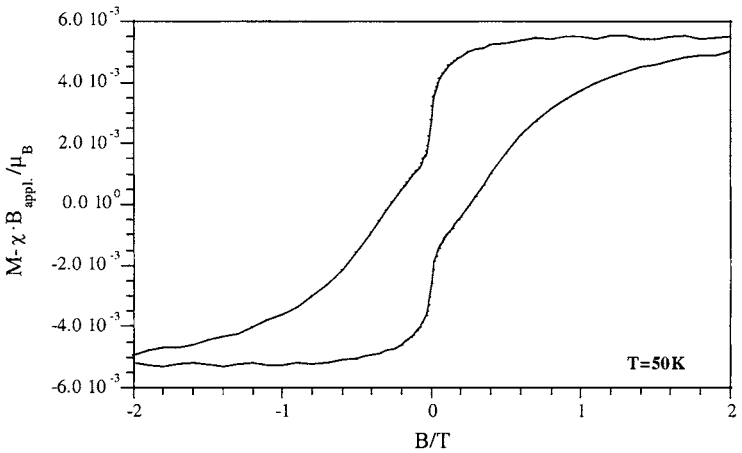

(b)

Figure 6. ZFC hysteresis loops obtained at three different temperatures below T_N for sample A once the linear contribution arising from the main antiferromagnetic framework has been subtracted. The narrowing occurring at low values of applied field has been interpreted as a result of a spin-flop transition along the *c*-axis.

of this transition explains the narrowing of the curves in figure 6, interpreted now as a hard reorientation of the weak ferromagnetic components occurring at the critical field B_1, and the hysteresis effects observed also in figure 6.

The small values of the induced moment obtained from the magnetization isotherms imply that the AFM–SF–SP transition involves only the weak ferromagnetic components arising from the DM anisotropic term rather than the staggered moments in the G-type AFM structure. Figure 8 shows a schematic diagram of the proposed evolution with applied field of the WFM moment assumed to be along *c*, from the antiferromagnetic arrangement at zero field (I) to the spin-flop phase (II) and, finally, the gradual rotation into the net weak ferromagnetic phase (III to V). Each horizontal line in the picture represents a perovskite block. We have shown in section 1 that a weak ferromagnetic moment arises on each MnO_2 plane as a result of the canting of the spins away from the perfect G structure. However, this moment cancels with that of the

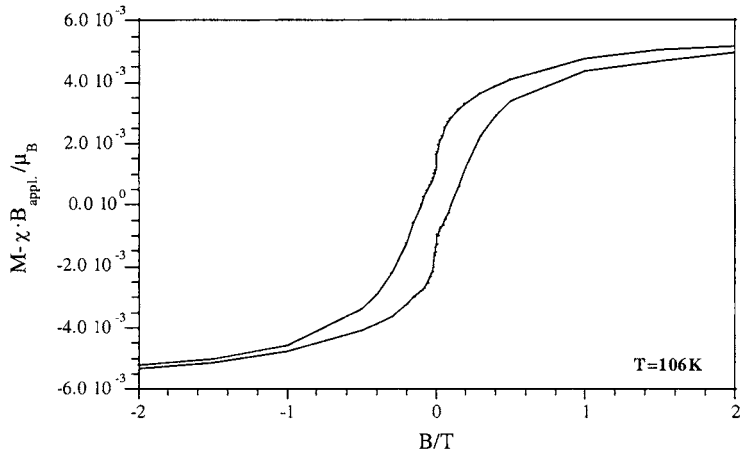

(c)

Figure 6. (Continued)

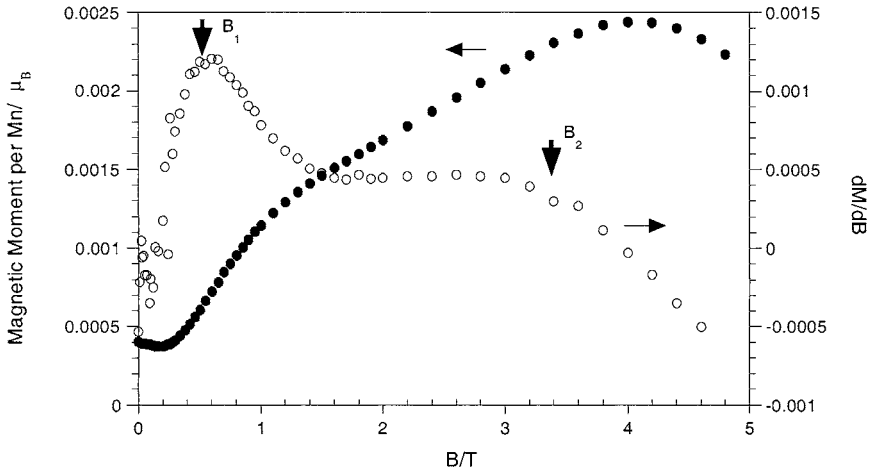

Figure 7. Initial magnetization curve collected at 5 K for sample B together with the differential susceptibility, χ_d, obtained numerically for the same data. The peak observed in χ_d together with the drop at high fields correspond to the expected behaviour for a Heisenberg antiferromagnet with weak anisotropy. B_1 represents the critical value of the applied field at which the transition into a spin-flop phase occurs and B_2 is the value for the transition into the saturated paramagnet regimen.

adjacent layer due to the antiferromagnetic character of the coupling J' within the perovskite block. Therefore, only an odd number of layers can give rise to a net WFM in each block. In $Ca_4Mn_3O_{10}$, $n = 3$. Now, the absence of weak ferromagnetism in zero field (see figure 2) must imply that the net moment on each perovskite block couples antiferromagnetically (i.e. $J'' < 0$) with that of the adjacent blocks. The result can be considered as a two-sublattice AFM arrangement of the WFM moments of the individual blocks along c ((I) in figure 8). Therefore, the spin-flop transition can be understood as the applied field overcoming the weak anisotropy introduced by J''. As B_{appl} is increased, the crystallites with the c-axis oriented along the direction of the magnetic field undergo the transition described above and give rise to the observed magnetization.

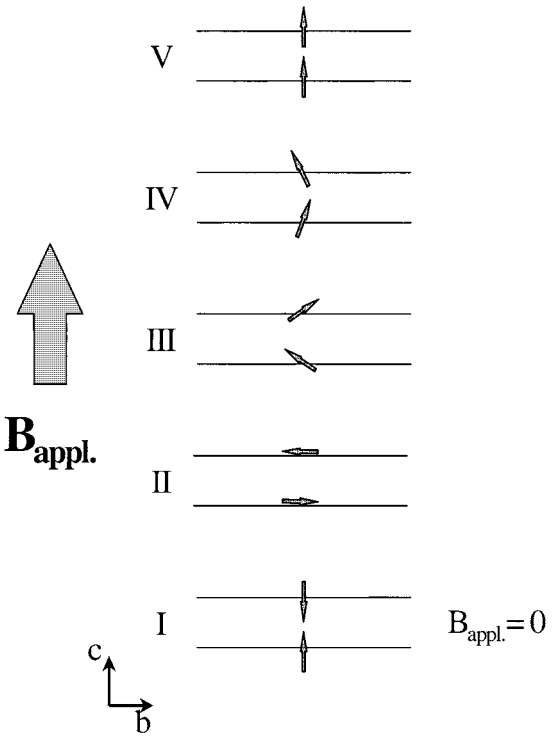

Figure 8. Schematic representation of the evolution of the weak ferromagnetic component with increasing applied magnetic field along c within each perovskite block. At zero field the weak antiferromagnetic component lies antiferromagnetically due to $J' < 0$ (I). Once the magnitude of the field reaches a certain critical value B_1 the system evolves into a spin-flop phase with the spins perpendicular to the field (II). A further increase in B induces a gradual spin rotation into the saturated paramagnetic regime (III to V).

In figure 7, the transition appears as a continuous change in magnetization and a rather broad peak in χ_d because of the polycrystalline character of our sample. The first-order nature is found to disappear as the angle between the applied field and the easy axis (which should be zero in the ideal case) increases above a certain value [55]. Instead, a gradual rotation occurs which smears the change in magnetization. The broad distribution of orientations with respect to the applied field occurring in a polycrystalline sample can hence account for the broad transition we observe. Demagnetization effects, which cannot be taken into account in a powder sample with a distribution of crystallite sizes and shapes, are known as well to mask the first-order nature of the transition [45]. The transition into the weak ferromagnetic phase ((III) to (V) in figure 8) is of second order and hence a discontinuity in χ_d, smeared again by the nature of the sample, is observed at a critical value B_2.

The proposed evolution of the weak ferromagnetic component with increasing applied field could account for the paramagnetic-like tail observed in the thermal dependence of the molar susceptibility of sample A at temperatures below 20 K in $B_{appl} = 0.01$ T (figure 2(a)). As the field increases this tail becomes predominant in both A and B samples and, in $B_{appl} = 5$ T the behaviour resembles that of a paramagnet for the whole temperature range below T_N. Figure 9 shows the temperature evolution of the molar susceptibility at $B_{appl} = 5$ T for sample B. Although the WFM jump can still be observed, the susceptibility increases in a

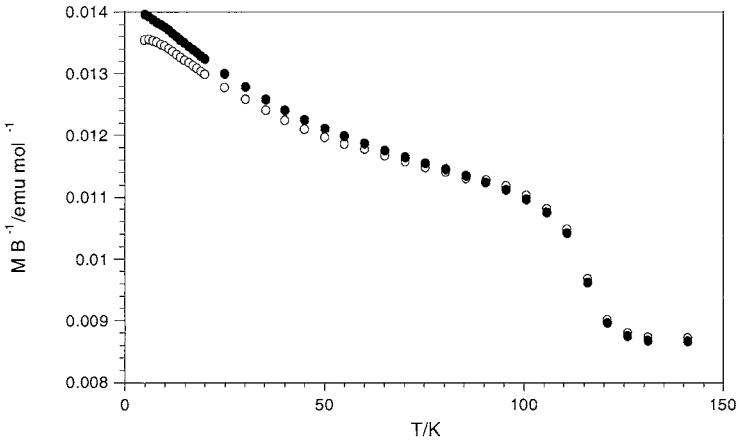

Figure 9. Temperature dependence of the molar magnetic susceptibility for sample B of $Ca_4Mn_3O_{10}$ in a field of 5 T. Filled and empty symbols are used to indicate field-cooled (FC) and zero-field-cooled (ZFC) data respectively. Although the WFM jump can still be observed, the susceptibility increases in a paramagnetic-like way from $T \leqslant T_N$.

paramagnetic-like way from temperatures immediately below T_N, consistent with the idea that the phase (V) is a saturated paramagnet rather than a true ferromagnet [45].

3.4. Spin-glass-type behaviour at low temperatures: disorder of the WFM moment

It is difficult to establish the origin of the drop in magnetization observed in the temperature range $20 < T\ (\mathrm{K}) < 50$ in figure 2(a). This drop is evidence for a more complex behaviour than expected for a conventional weak ferromagnet. In order to obtain a deeper insight into the nature of this phase, we have studied the relaxation with time of the thermoremanent magnetization (TRM).

A decrease in magnetization on cooling beyond saturation is normally evidence of a so-called re-entrant transition [56–60] in which a ferromagnetic system with substantial structural randomness disorders into a spin-glass-like phase as temperature is progressively lowered below the Curie point. The time-dependent behaviour is different for both regimes and, hence, relaxation experiments above and below the transition can provide a great deal of information about the evolution of the magnetization with decreasing temperature. A stretched exponential form of the time decay of the thermoremanent magnetization is specific to spin glass freezing [61–65] whereas for a pure ferromagnet, approach to equilibrium is much faster and it is described by a power law [66].

Measurements were performed on both types of sample, A and B. The results are displayed in figures 10 and 11 in semi-log plots. As expected, the magnitude of the TRM at $t = 0$ decreases with increasing temperature, and is comparable for the two different samples at similar temperatures.

Sample B, figure 10, shows a marked difference between the behaviour at 20 and 80 K. At 20 K it shows a very slow approach to equilibrium in a way similar to that in a pure spin glass [60]. The remanent magnetization can be represented over the entire time domain by a stretched exponential function superposed on a time-independent baseline of the form

$$\mathrm{TRM}(t) = M_0 + M_1 \exp\left(-\left(\frac{t}{\tau}\right)^{1-n}\right) \tag{5}$$

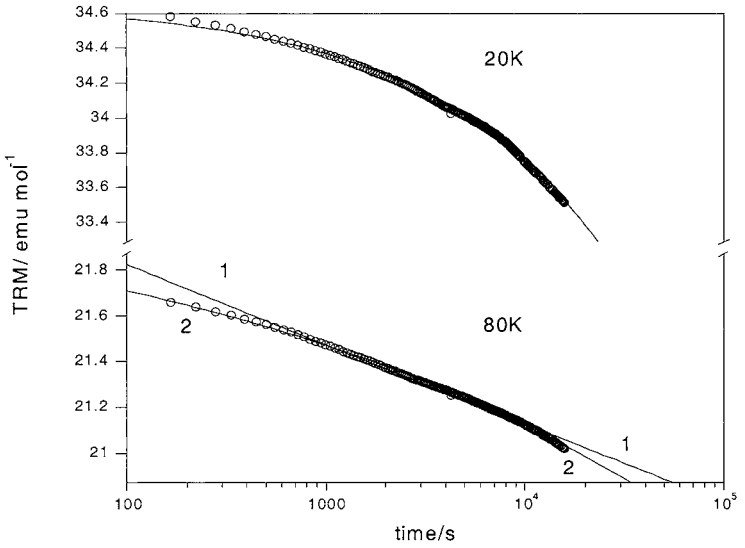

Figure 10. Thermoremanent magnetization (TRM) decay for sample B at two different temperatures below the Néel point. The line on the 20 K data represents the best fit to a stretched exponential function (equation (6)). Lines 1 and 2 on the 80 K data represent the fit to a stretched exponential and a power law function respectively.

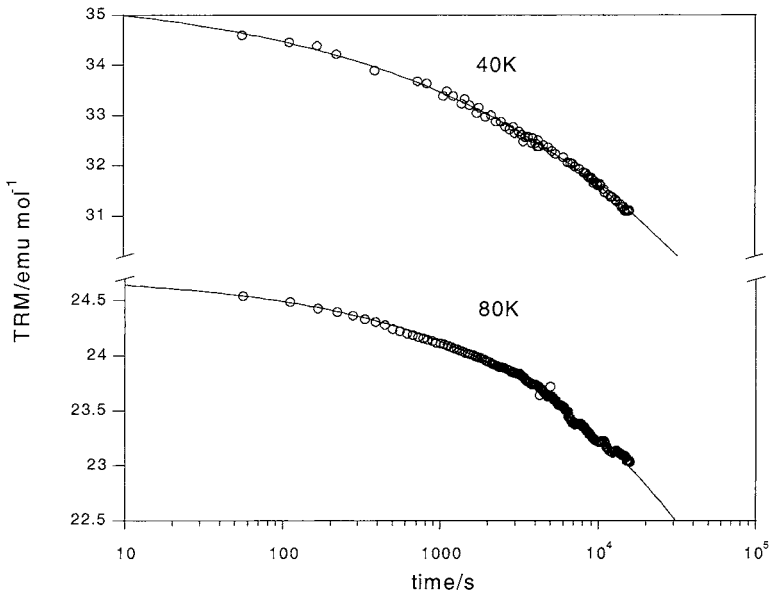

Figure 11. Thermoremanent magnetization (TRM) decay for sample A at two different temperatures below the Néel point. The lines represent the fit to a stretched exponential function (equation (6)) in both cases.

where $\tau = 3.7 \times 10^6$ s is the time constant of the relaxation process, and $M_1 + M_0 = 34.66$ emu mol$^{-1} \simeq$ TRM(0). From the fit we obtain a value of $n = 0.50$. The obtained values of τ and n are similar to those reported in other spin-glass or reentrant systems [60, 61, 67].

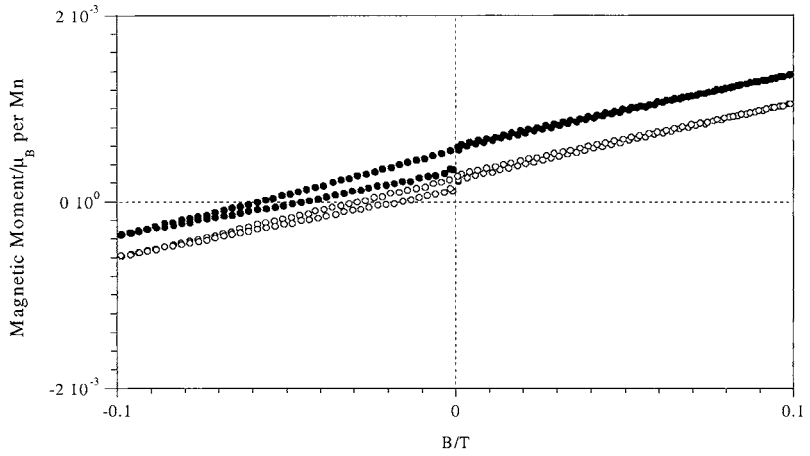

Figure 12. FC $M(H)$ measurements collected at 10 K for a type-A sample under $B = 10^{-3}$ T (open circles) and 2×10^{-3} T (filled circles). The shift of the hysteresis loop along the magnetization axis evidences the presence of unidirectional anisotropy and is characteristic of spin-glass behaviour.

At 80 K, in contrast, relaxation is much faster during the early stages and slows down in the later decades. The data are still fitted by equation (5) (line 2 in figure 10). The fit yields $\tau = 1.5 \times 10^{10}$ s, $n = 0.82$ and $M_1 + M_0 = 22.19$ emu mol^{-1}. However, the large change in τ occurring between 20 and 80 K casts a doubt on the validity of the fit at the higher temperature (we are not aware of any time decay study of the TRM of a spin glass yielding such a large value of the relaxation constant). In fact, it seems to indicate a change in the nature of the spin dynamics between the two temperatures. A crossover from a stretched exponential to a power law fit of the time decay of the TRM has been reported for reentrant systems at the transition from RSG $\rightarrow$ FM on warming up [60, 67]. Line 1 in figure 10 shows the attempt to fit the data at 80 K with a power law TRM$(t) \propto t^{-\beta}$. The fit is clearly much worse than that of the stretched-exponential function.

Data collected for sample A at 40 and 80 K are displayed in figure 11. A similar qualitative behaviour is observed at both temperatures. A stretched-exponential function fits the two curves giving $\tau = 1.8 \times 10^6$ s and $n = 0.70$ at 40 K and $\tau = 2.3 \times 10^6$ s and $n = 0.60$ at 80 K. These values are of the same order of magnitude as those found in well characterized spin glasses [60].

Figure 12 shows FC magnetization measurements carried out on a type A sample at 10 K for two different cooling fields ($B = 10^{-3}$ and 2×10^{-3} T). The shift of the FC hysteresis loops along the magnetization axis is characteristic of spin-glass systems [68].

We may conclude from the results above that the low-temperature phase displays a spin-glass-like character for both samples. However, whereas for sample A a simple spin-glass-type behaviour extends to the highest measured temperature, for sample B there is a change in dynamics as demonstrated by the large change in the relaxation rate between 20 and 80 K.

The slow spin dynamics found at low temperatures can be interpreted by considering that the weak ferromagnetic moment in each MnO_2 plane is itself disordered at all temperatures below T_N. The origin of this behaviour in $Ca_4Mn_3O_{10}$ cannot be determined from the present measurements. Rouco [33] and Mira [34] have proposed that an inhomogeneous distribution of the structural distortions that give rise to the weak ferromagnetic component cause the spin-glass-type behaviour in Y_2CuO_4 and Gd_2CuO_4 respectively. According to this explanation, the short-range character of the distortion leads to finite-size magnetized clusters, where a cluster

is defined as a local uniformly distorted region in each plane with a unique direction for the net magnetization. The presence of these clusters would explain the spin-glass characteristics (strong irreversibility, shifted FC hysteresis loops and slow magnetization decay) observed in our system for $T \leqslant T_N$. High-resolution neutron diffraction studies of sample A showed hkl-dependent broadening of some reflections, indicating the existence of crystallographic defects that could well be the origin of the proposed inhomogeneous distribution of the magnetization.

The saturated paramagnetic nature of the low-temperature phase is consistent with the observation of a paramagnetic tail and may be responsible for the slow dynamics (figure 9). When the field is switched off at the experimental temperature in the relaxation experiments, phase (V) in figure 8 would relax following a vertical line in the theoretical H–T phase diagram proposed by de Jongh [45] crossing the spin-flop region where the spins would undergo a gradual transition back into the AFM phase. However, this model does not provide an explanation for the different behaviour observed for the two samples, nor for the two temperature regimes of sample B. Our lack of knowledge of the detailed H–T phase diagram for this specific system prevents our knowing where the system lies at the initial stage of the TRM measurements.

4. Conclusions

The dc-magnetization measurements carried out in this work show a weak ferromagnetic (WFM) transition occurring at T_N for samples of $Ca_4Mn_3O_{10}$ synthesized under different oxygen pressure. The fact that the onset of weak ferromagnetism is independent of the synthetic conditions allows us to rule out a double-exchange origin for the magnetic order. The weak ferromagnetic component arises from a slight canting of the antiferromagnetic sublattices due to an antisymmetric Dzyaloshinskii–Moriya term in the Hamiltonian. The resulting WFM component associated with each MnO_2 plane is hidden at zero field by the antiferromagnetic character of the inter-block exchange constant. The application of a magnetic field overcomes the weak anisotropy along the c-axis, and the system undergoes a successive AFM–SF–FM (SP) transition involving just the WFM component, which gives rise to the net weak moment we observe below the Néel temperature in the thermomagnetic measurements.

Above the transition temperature the susceptibility shows a weak temperature dependence and is indistinguishable for samples annealed both under mild and strong oxidizing conditions. The presence of a broad maximum at $T \sim 155$ K, characteristic of 2D AFM systems, underlines the presence of antiferromagnetic correlations confined to the ab planes above the transition temperature. We therefore propose that $Ca_4Mn_3O_{10}$ displays behaviour intermediate between 2D and 3D. The fit of the sublattice AF staggered magnetization to a scaling power law in a wide temperature range yields an exponent $\beta \sim 0.28$ in agreement with this picture. The applied magnetic field is also responsible for the small ferromagnetic component observed at temperatures above the transition as it induces an ordering of the ferromagnetic moments which arise from the DM interaction within the finite 2D correlated regions that exist at $T \geqslant T_N$. The existence of this ferromagnetic component may be responsible for persistence of negative magnetoresistance to temperatures above T_N for this compound.

The behaviour below the transition temperature is strongly dependent on the annealing treatment as well as on the applied field. Whereas for samples annealed under high P_{O_2} the magnetization remains saturated on cooling to 5 K, for those annealed under $P_{O_2} = 1$ atm it decreases after saturation. TRM relaxation measurements below T_N show slow relaxation characteristic of spin-glass systems for both types of sample although in the case of sample B there is a change in spin dynamics at higher temperatures (still below T_N). This behaviour is tentatively explained by the presence of regions (clusters) of coherently aligned DM vectors, the

direction of which varies from cluster to cluster. This disorder can explain the spin-glass-like behaviour at $T \leqslant T_N$. An alternative explanation could come from the proposed paramagnetic nature of the 'weak ferromagnetic phase'. The relaxation of this phase once the field has been switched off in the TRM decay experiments, evolving through the spin-flop phase in the phase diagram, could explain the slow dynamics we observe for this system.

Acknowledgments

JL would like to thank the Basque government (Departamento de Educacion, Gobierno Vasco) for financial support in the form of a PhD studentship.

References

[1] Kusters R M, Singleton J, Keen D A *et al* 1989 *Physica* B **155** 1989
[2] von Helmholt R, Wecker J, Holzapfel B *et al* 1993 *Phys. Rev. Lett.* **71** 2331
[3] Jonker H and van Santen J H 1950 *Physica* **16** 337
[4] Jonker H and van Santen J H 1953 *Physica* **19** 120
[5] Zener C 1951 *Phys. Rev.* **82** 403
[6] Millis A J, Littlewood P B and Shaiman B I 1995 *Phys. Rev. Lett.* **74** 5144
[7] Roder H, Zang J and Bishop A R 1996 *Phys. Rev. Lett.* **76** 1356
[8] Millis A J, Shaiman B I and Mueller R 1996 *Phys. Rev. Lett.* **77** 175
[9] Shimakawa Y, Kubo Y and Manako T 1996 *Nature* **379** 53
[10] Subramanian M A, Toby B H, Ramirez A P *et al* 1996 *Science* **273**
[11] Ruddlesden S N and Popper P 1958 *Acta Crystallogr.* **11** 541
[12] Moritomo Y, Asamitsu A, Kuwahara H *et al* 1996 *Nature* **380** 141
[13] Bao W, Chen C H, Carter S A *et al* 1996 *Solid State Commun.* **98** 55
[14] Moritomo Y, Tomioka Y, Asamitsu A *et al* 1995 *Phys. Rev.* B **51** 3297
[15] Maignan A, Martin C, van Tendeloo G *et al* 1998 *J. Mater. Chem.* **8** 2411
[16] Asano H, Hayakawa J and Matsui M 1996 *Appl. Phys. Lett.* **68** 3638
[17] Asano H, Hayakawa J and Matsui M 1997 *Appl. Phys. Lett.* **70** 2303
[18] Asano H, Hayakawa J and Matsui M 1997 *Phys. Rev.* B **56** 5395
[19] Battle P D, Blundell S J, Green M A *et al* 1996 *J. Phys.: Condens. Matter* **8** L427
[20] Nur N H, Kim J T, Yoo K H *et al* 1998 *Phys. Rev.* B **57** 10 740
[21] Felser C, Seshadri R, Leist A *et al* 1998 *J. Mater. Chem.* **8** 787
[22] Goodenough J B 1955 *Phys. Rev.* **100** 564
[23] Kanamori J 1959 *J. Phys. Chem. Solids* **10** 87
[24] MacChesney J B, Williams H J, Potter J F *et al* 1967 *Phys. Rev.* B **164** 779
[25] Rossell H J, Goodman P, Bulcock S *et al* 1996 *Aust. J. Chem.* **49** 205
[26] Witte N S, Goodman P, Lincoln F J *et al* 1998 *Appl. Phys. Lett.* **72** 853
[27] Asano H, Hayakawa J and Matsui M 1997 *Appl. Phys. Lett.* **71** 844
[28] Asano H, Hayakawa J and Matsui M 1998 *Phys. Rev.* B **57** 1052
[29] Mihut A I, Spring L E, Bewley R I *et al* 1998 *J. Phys.: Condens. Matter* **10** L717
[30] Briatico J, Alascio B, Allub R *et al* 1996 *Phys. Rev.* B **53** 14 020
[31] Battle P D, Green M A, Lago J *et al* 1998 *Chem. Mater.* **10** 658
[32] Koehler W C, Wollan E O and Wilkinson M K 1960 *Phys. Rev.* **118** 58
[33] Rouco A, Obradors X, Tovar M *et al* 1994 *Phys. Rev.* B **50** 9924
[34] Mira J, Rivas J, Fiorani D *et al* 1995 *Phys. Rev.* B **52** 16 020
[35] Steren B, Fainstein A, Tovar M *et al* 1993 *J. Appl. Phys.* **73** 5710
[36] Fawcett I D, Sunstrom IV J E, Greenblatt M *et al* 1998 *Chem. Mater.* **10** 3643
[37] Maignan A, Martin C, Damay F *et al* 1998 *Phys. Rev.* B **58** 2758
[38] Dzyaloshinskii I 1958 *J. Phys. Chem. Solids* **4** 241
[39] Moriya T 1960 *Phys. Rev.* **120** 91
[40] Levy P M and Fert A 1981 *Phys. Rev.* B **23** 4667
[41] Stepanov A A, Wyder P, Chattopadhyay T *et al* 1993 *Phys. Rev.* B **48** 12 979
[42] Coffey D, Bedell K S and Trugman S A 1990 *Phys. Rev.* B **42** 6509
[43] Lines M E 1967 *Phys. Rev.* **164** 736

[44] Lines M E 1970 *J. Phys. Chem. Solids* **31** 101
[45] de Jongh L J and Miedema A R 1974 *Adv. Phys.* **23** 1
[46] Goodenough J B 1967 *Phys. Rev.* **164** 785
[47] Rushbrooke G S and Wood P J 1958 *Mol. Phys.* **1** 257
[48] Rushbrooke G S and Wood P J 1963 *Mol. Phys.* **6** 410
[49] Rushbrooke G S and Wood P J 1974 *Phase Transitions and Critical Phenomena* ed C Domb and M S Green (New York: Academic)
[50] A value of $J/k_B \sim 52$ K was found by Lines (see Lines M E 1970 *J. Phys. Chem. Solids* **31** 101) using a series expansion analysis of the high temperature susceptibility starting with an exchange Hamiltonian of the type $\sum J(S_i S_j)$, in contrast to that used by de Jongh and Rushbrooke, which contains a $2J$ term. Therefore, this value would correspond to $J/k_B \sim 26$ K using de Jongh's Hamiltonian.
[51] White T R, Glaunsinger W S, Horowitz H S *et al* 1979 *J. Appl. Phys.* **50** 1926
[52] Bramwell S T and Holdsworth P C W 1993 *J. Phys.: Condens. Matter* **5** L53
[53] Bramwell S T and Holdsworth P C W1993 *J. Appl. Phys.* **73** 6093
[54] Bramwell S T, Day P, Hutchings M T *et al* 1986 *Inorg. Chem.* **25** 417
[55] Fries T, Shapira Y, Palacio F *et al* 1998 *Phys. Rev.* B **56** 5424
[56] Campbell I A and Senoussi S 1992 *Phil. Mag.* B **65** 1267
[57] Kunkel H P and Williams G 1988 *J. Magn. Magn. Mater.* **75** 98
[58] Berndt A G, Chen X, Kunkel H P *et al* 1995 *Phys. Rev.* B **52** 10 160
[59] Srivastava B K, Krishnamurthy A, Ghose V *et al* 1994 *J. Magn. Magn. Mater.* **132** 124
[60] Sinha G, Chatterjee R, Uehara M *et al* 1996 *J. Magn. Magn. Mater.* **164** 345
[61] Roshko R M and Ruan W 1992 *J. Magn. Magn. Mater.* **104–107** 1613
[62] Lundgren L, Nordblad P and Svedlindh P 1986 *Phys. Rev.* B **34** 8164
[63] Chamberlin R V 1985 *J. Appl. Phys.* **57** 3377
[64] Fisher D S and Huse D A 1988 *Phys. Rev.* B **38** 373
[65] Fisher D S and Huse D A 1988 *Phys. Rev.* B **38** 386
[66] Gunton J D, San Miguel M and Sahui P S 1983 *Phase Transitions and Critical Phenomena* vol 8, ed C Domb and J L Lebowitz (New York: Academic)
[67] Mitchler P, Roskho R M and Ruan W 1992 *J. Physique* I **2** 2299
[68] Fischer K H and Hertz J A 1991 *Spin Glasses* (Cambridge: Cambridge University Press)